Received: 20 August 2021 | Revised: 31 October 2021 | Accepted: 23 November 2021

DOI: 10.1002/1438-390X.12112

Population Ecology WILEY

ORIGINAL ARTICLE

Demographic and growth patterns of *Pentaclethra macroloba* (Willd.) Kuntze, a hyperdominant tree in the Amazon River estuary

Adelson Rocha Dantas[1,2] | **Marcelino Carneiro Guedes**[2] | **Ana Cláudia Lira-Guedes**[2] | **Jochen Schöngart**[1] | **Maria Teresa Fernandez Piedade**[1]

[1]Programa de Pós-graduação em Ecologia, Instituto Nacional de Pesquisas da Amazônia, Manaus, Brazil

[2]Departamento de Recursos Florestais, Empresa Brasileira de Pesquisa Agropecuária/Embrapa Amapá, Macapá, Brazil

Correspondence
Adelson Rocha Dantas, Departamento de Ecologia, Programa de Pós-graduação em Ecologia, INPA-V8, Av. André Araújo 97, Adrianópolis, Manaus, Brazil.
Email: adelson.dantas@yahoo.com.br

Funding information
Conselho Nacional de Desenvolvimento Científico e Tecnológico, Grant/Award Number: 142316/2016-4; Empresa Brasileira de Pesquisa Agropecuária, Grant/Award Number: 02.13.07.007.00.00

Abstract

Little is known about the life history and environmental factors that regulate the growth rate of hyperdominant trees in flooded Amazonian forests. *Pentaclethra macroloba* is a hyperdominant tree, and it is widely explored in the Amazon, because its seed oil is a powerful herbal medicine. We evaluated the demographic structure and growth patterns of *P. macroloba* and tested the effect of the Amazon River flood pulse on its growth. We modeled the growth and determined the age of *P. macroloba* by analyzing the growth rings of 30 monitored trees in relation to hydroclimatic variables. We also inventoried 240 juvenile and 2072 adult trees arranged in a clustered pattern. The diametric distribution pattern of the juvenile and adult trees was exponential and log-normal, respectively. The trees were found to be up to 102 years old, and 47% of them grew freely toward the canopy. Peak growth in height and diameter occurred at 24 (61.7 cm year^{-1}) and 46 (9.38 mm year^{-1}) years, respectively. *Pentaclethra macroloba* showed cambial dormancy during the seasonal peak of rainfall ($R^2 = 0.41$; $t = -2.62$; $p < 0.01$) and flooding of the Amazon River ($R^2 = 0.47$; $t = -3.01$; $p < 0.01$). Increases in rainfall and flood level of the river in the rainy season control the growth rate of *P. macroloba*, making it a seasonal process. The demographic and growth patterns of *P. macroloba* respond to the environmental heterogeneity of the estuarine floodplain forest and also reflect its life history over time.

KEYWORDS

flood pulse, floodplain forest, growth rings, pracaxi, seasonality

1 | INTRODUCTION

Flooded areas of the Amazon are constituted by a complex interconnected system of habitats formed by variations in topography and flood regimes. In the estuarine region of the Amazon River and its white water tributaries, the floodplain forests occupy approximately 199,281 km^2 (Junk & Piedade, 2010). The Amazon estuary has two daily flood cycles or a predictable polymodal flood pulse (Junk et al., 2011), as the tide of the Atlantic Ocean influences this region. The flood dynamics of Amazon floodplain forests act as an environmental filter that selects the species most adapted to the fluctuations of this environment (Luize et al., 2018).

The tree species *Pentaclethra macroloba* (Willd.) Kuntze is well adapted to the daily flood of the Amazon estuary, as it has a high population density in this estuarine environment (Carim et al., 2016) and it is one of 10 species considered hyperdominant in the Amazon (ter Steege et al., 2020). *Pentaclethra macroloba*, known by the popular name "pracaxi" or "pracaxizeiro" in Brazil, belongs to the Fabaceae family (Dantas et al., 2017). In the Amazon estuary, this species has a mean of 13 m height and 23 cm diameter (Dantas et al., 2017). The leaf is bipinnate, inflorescence is a terminal spike, fruit is a dehiscent dry legume and the deltoid seeds have mechanisms adapted to hydrochoric dispersal (Dantas, Guedes, Vasconcelos, et al., 2021).

Hartshorn (1983) considers the existence of three large populations of *P. macroloba* in Latin America. The first population, widely studied, is concentrated in Costa Rica, mainly in the *La Selva* Forest Reserve, where the species presents monodominance. The second population is concentrated in the extension from Panama to Colombia. The third and last population is located in the Northeast of the Brazilian Amazon and for it, the natural history is little known. The species occurs in Guatemala, Costa Rica, Panama, Colombia, Venezuela, Trinidad and Tobago, Guiana, French Guiana, Suriname, and Brazil (Dantas, Guedes, Vasconcelos, et al., 2021).

The trunk bark of *P. macroloba* has terpenoid saponins that have anti-hemorrhagic action against the venom of *Bothrops* vipers (da Silva et al., 2007). The main product used from *P. macroloba* is the oil extracted from the seeds, considered a potent herbal medicine for the healing of diabetic ulcers (Simmons et al., 2015), wounds, and burns (Banov et al., 2014). There are also reports of traditional use to treat snake bites, muscle pain, and wounds caused by leishmaniasis (Sarquis et al., 2019).

Pracaxi oil can be considered an essential product of socio-biodiversity, as the oil extraction is a source of extra income for riverine populations. People from traditional communities sell the oil to the cosmetic industries, or at local markets for R$100/l ($18). Cosmetic industries have shown great interest in the pracaxi oil due to its high concentration of fatty acids that have an emollient action on skin hydration (Costa et al., 2014). The number of patented pharmaceutical and cosmetic products based on pracaxi oil is currently growing, both in the national and international market (Oliveira et al., 2020). With this growing demand, the sustainability of the seed collection becomes concern, as larger-scale seed extraction may reduce the sustainability of wild populations.

A knowledge of the demographic patterns and the ecological factors that influence the population structure is useful to setting up sustainable management actions for this species. In floodplain forests, the amplitude and duration of flooding are preponderant factors that influence the structure, physiology (Parolin et al., 2010), richness, diversity, and spatial distribution pattern of forest communities (Ferreira & Stohlgren, 1999). Many species from flooded areas of the Amazon synchronize their fruiting with the flooding period of the Amazon rivers (Kubitzki & Ziburski, 1994; Schöngart et al., 2002), favoring seed dispersal by water and fishes (Parolin et al., 2013).

The monomodal flood pulse of Central Amazonia, that can reach up to 10 m in height and lasting up to 270 days, has a drastic effect on plant metabolism (Parolin et al., 2004) and tree growth (Schöngart et al., 2002). The trees of this environment have cambial dormancy during the river's peak flood and they resume their growth in the dry season (Schöngart et al., 2002). The physiological stress caused by floods in the plant can be observed in the differentiation of the anatomical wood structures that appear as annual rings (Worbes & Fichtler, 2010). However, in the Amazon estuary, where the flood regime is daily and of short duration, knowledge of the adaptive responses of trees to the conditions of this environment is still incomplete.

We sought to assess the demographic and the life history parameters of *P. macroloba* to explain its hyperdominance in the Amazon and to assist in public management policies and the conservation of its natural resources. Our hypothesis is that the Amazon River flood pulse acts as a physiological stressor regulating the growth rate of *P. macroloba*.

2 | MATERIALS AND METHODS

2.1 | Site description

The study was carried out in the floodplain forests of the Fazendinha Environmental Protection Area (APA), a reserve of 136.59 ha, and in the Mazagão Experimental Field (CEM), an area of 55.95 ha (Figure 1). Both areas are located in Amapá State, Brazil. The APA is a conservation unit for sustainable use located in Macapá city 00°03′04,24″S and 51°07′42,72″W. The CEM belongs to the Brazilian Agricultural Research Corporation, located in Mazagão city 00°02′33″S and 51°15′24″W.

The estuarine forests in this study are influenced by the tide of the Amazon River, characterized by the occurrence of two flood daily pulses (Junk et al., 2011). Flood waters can reach heights of up to 60 cm on tree trunks inside the forest (Dantas, Guedes, Lira-Guedes, & Piedade, 2021) or up to 4 m in the rainy season in the mouth of the Amazon River (Cunha et al., 2017). These areas are formed by a rich system of channels and

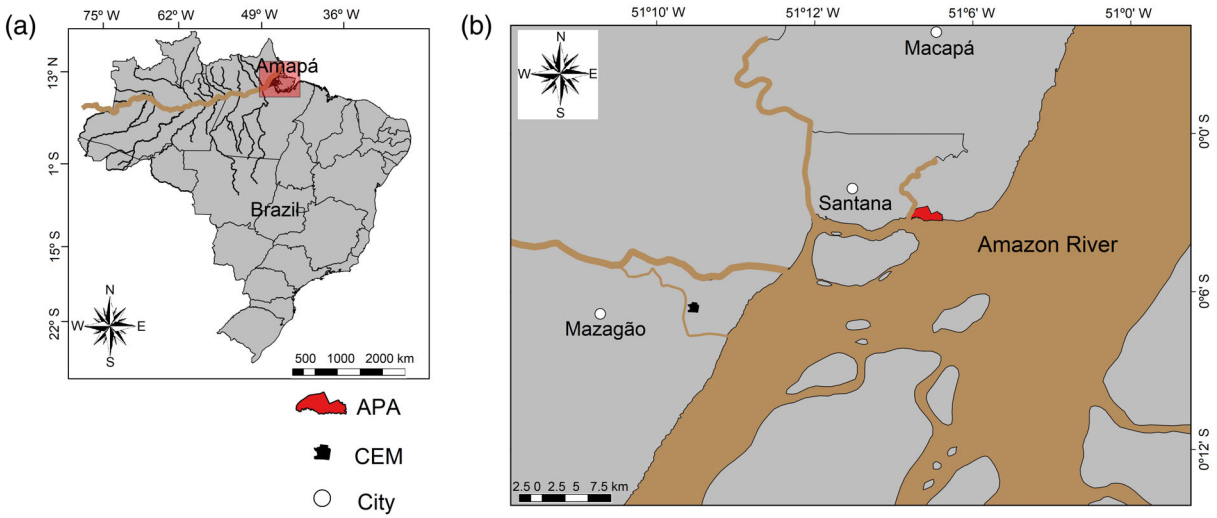

FIGURE 1 Two populations of *Pentaclethra macroloba* located in the Fazendinha Environmental Protection Area (APA) and in the Mazagão Experimental Field (CEM), in the region of the Brazilian Amazon estuary (a), Amapá State (b) [Color figure can be viewed at wileyonlinelibrary.com]

streams that regulate the entry and exit of water from the Amazon River.

In the APA, the area is flat, with small slopes, and the flood waters are evenly distributed throughout the area. In CEM, the various slopes of the soil result in different flood gradients, forming high and low floodplain environments (Wittmann et al., 2002). In the low floodplain, the flooding reaches the soil daily and up to 60 cm on the tree trunks during the rainy season. In the high floodplain, the soil has a slope from 3 to 3.5 m high, hindering the entry of the daily tide in this environment. However, the high floodplain is partially flooded in the rainy season, where flooding level reaches 10 cm on the tree trunks (Dantas et al., 2020).

The climate system in the region is Am type, rainy tropical (Alvares et al., 2014). In Amapá State, the rainy season starts in December, and the rains are concentrated in March, when the peak of rainfall remains above 60 mm until August. The dry season starts in September when the rainfall is below 60 mm monthly. The mean annual rainfall is 2460 mm and the mean maximum temperature varies from 30 to 32°C (de Vilhena et al., 2018).

The soils are Melanic Gleisols, characteristic of the floodplain region of the Amazon estuary. These soils are silty texture and with predominance of smectite, illite, kaolinite, goethite, anatase, and quartz (Pinto, 2014).

The vegetation is classified as Dense Alluvial Ambrophilous Forest (IBGE, 2012). The five most abundant species, among the 98 registered species, are: *Mora paraensis* (Ducke) Ducke (Fabaceae), *Astrocaryum murumuru* Mart. (Arecaceae), *P. macroloba* (Willd.) Kuntze (Fabaceae), *Carapa guianensis* Aubl. (Meliaceae), and *Matisia paraensis* Huber (Malvaceae; Carim et al., 2016).

2.2 | Data collection

2.2.1 | Inventory of the adult trees

The demographic parameters of the adult trees of *P. macroloba* were determined based on an inventory performed in 136.59 ha of the APA, in the period from September to November 2017. All trees of *P. macroloba* with diameter at breast height (dbh) ≥5 cm present in the study area were inventoried. Tree dbh was measured with a tape measure, and trees were identified numerically with zinc tags. The coordinates of all individuals were obtained with a GPS device (Garmin 60CSx) of ±3 m accuracy.

The total height of each tree was measured with a laser rangefinder (Bosch—GLM 40) of 1.5 mm accuracy and with reach of 40 m. In obtaining height, the observer positioned himself below the tree's crown, close to the trunk, and visualized the last branch to launch the laser toward it. The final height of the tree was estimated from the sum of the observer height (with the arm extended) and the measurement captured on tape measure.

Qualitative data evaluated were: (a) reproductive status: presence or absence of fruits or vestiges of reproductive structures in the crown—the inventory was carried out during the flowering period and emergence of the first fruits, and (b) canopy position, classified as: dominant (the tree occupies the upper layer of the canopy, where the crown is completely exposed to light), codominant (the tree occupies the intermediate layer of the

canopy, where the crown is not entirely exposed to light, due to partial shading of neighboring dominant trees) and suppressed (the tree occupies the understory of the forest, where there is no incidence of direct light in the crown; Dawkins, 1958).

2.2.2 | Regeneration sampling

Natural regeneration was evaluated in two 100 m × 100 m (1 ha) plots each, installed at the same topographic level and separated by 177 m of distance. The inventory was carried out in April 2019 at APA, and all seedlings with height <1.60 m and all saplings with height ≥1.60 m and diameter <5 cm were measured (Klimas et al., 2007), tagged, and georeferenced. Seedling diameter was measured at the soil height (dsh) and sapling at the dbh with the aid of a digital caliper (Carbografite® model 150, accuracy of 0.01 mm). Height was measured with a tape measure.

2.2.3 | Sampling of the radial wood

We determined the age and growth patterns of 38 trees selected in the APA. Our criterion was to select trees with a good phytosanitary aspect, with straight trunk and dbh > 5 cm from different diametric classes. Trees with large buttresses, eccentric trunk and with anomalies in the trunk were avoided. Two wood samples were obtained per tree, with the aid of an increment borer (Haglöf Sweden®, 5.15 mm in diameter and 400 mm in length) at dbh. The samples were sent to the Embrapa Amapá Dendrochronology Laboratory, where they were fixed on a wooden support and polished with sandpaper of different grits (100, 200, 400, and 1500 grains/mm^2) for better visualization of the growth rings.

Growth rings were visualized with the aid of a stereomicroscope (Leica EZ4D) with an attached camera and the images of each sample were obtained with a 20× magnification. The images were saved in the ".jpg" format with a resolution of 1200 dpi and calibrated in the 1 mm scale. The growth ring width was measured using the ImageProPlus software (version 4.5.0.29).

2.2.4 | Monitoring of diametric growth and hydrometeorological variables

In the CEM, the diametric growth of *P. macroloba* was evaluated through dendrometric bands installed in June 2018 on the trunk of 30 trees at breast height. We selected trees of different diametric classes, dominant and codominant in the canopy and in different topographic levels (10 trees in the high floodplain and 20 in the low floodplain). After 1 month of dendrometer band adjustment, the readings of the diametric growth were measured monthly, with a digital caliper, until December 2019 (18 months).

Water level height was measured using white strings installed parallel to the trunk of each monitored tree (Dantas, Guedes, Lira-Guedes, & Piedade, 2021). The water, full of river sediment, stains the white string leaving the flood height recorded, facilitating the measurement with a tape measure. The monthly data of accumulated rainfall and maximum mean temperature were obtained from the Climatological Station of Macapá (INMET, 2019).

2.3 | Data analysis

2.3.1 | Demographic structure

The parameters of the demographic structure analyzed were: population density (Equation 1), diametric classes (Equation 2, suggested by Sturges, 1926) height classes, basal area (Equation 3), spatial distribution, and age group.

$$\mathrm{PD} = \frac{N}{A}, \tag{1}$$

$$C = 1 + 3.333\mathrm{LN}(N), \tag{2}$$

$$g_i = \frac{\pi.\mathrm{dbh}^2}{40000};\ G = \sum_{i=l}^{n} g_i, \tag{3}$$

PD = population density (ha^{-1}); N = total number of sampled individuals; A = total area sampled; C = number of diametric classes; LN = natural logarithm; g_i = basal area of individual i; π = pi number (approximate value of 3.141592); dbh = diameter at breast height measured at 1.30 m from the soil (40,000 = conversion value for meters when the dbh is in centimeters); and G = basal area of the population (m^2 ha^{-1}).

Geographical coordinates of each individual were used to describe the pattern of spatial distribution of the population through the univariate Ripley's K function (Ripley, 1981; Equation 4). In the univariate method, the null hypothesis is of complete spatial randomness (CSR). The $\widehat{K}(s)$ function must be transformed to the $\widehat{L}(s)$ function (Equation 5) for better visualization of the results graphically. The CSR hypothesis was tested by the Monte

Carlo test, with 1000 confidence envelopes of the Poisson pattern surrounding the distance vector s, down 5% and up 5%, of the transformed function $\widehat{L}(s)$ (Goreaud et al., 1997).

$$\widehat{K}(s) = \frac{1}{\widehat{\lambda}_N} \sum_{i=1}^{N} \sum_{j=1}^{N} W_I^1(x_1, x_j) I(||x_i - x_j|| < s), \quad es > 0, \tag{4}$$

$$\widehat{L}(s) = \sqrt{\frac{\widehat{K}(s)}{\pi}} - s, \tag{5}$$

$\widehat{K}(s)$ = expected number of events; $(\|x_i - x_j\|)$ = Euclidean distance between locations x_i and x_j; s = arbitrary distance vector; $W_I(x_1, x_j)$ = edge effect correction function that shows the proportion of the circumference with center x_i and radius $\|x_i - x_j\|$ that is outside the study region; $\widehat{\lambda}_N$ = number of trees divided by the area of the study region, being a non-vicious estimator of the process intensity; and $\widehat{L}(s)$ = is the result of the transformed function $\widehat{K}(s)$.

To verify the degree of detachment of the population from the expected random distribution, the aggregation index R (Equation 6) was calculated by the mean distance of the nearest neighbor tree (Clark & Evans, 1954):

$$R = \frac{\overline{r}_A}{\overline{r}_E}, \tag{6}$$

$\overline{r}_A$ = mean distance from the nearest neighbor = $\frac{\sum r_i}{N}$; r_i = distance of the nearest neighbor to individual i; $\overline{r}_E$ = expected distance to the nearest neighbor under CSR = $\frac{1}{\sqrt[2]{\mu}}$; and μ = tree density.

The random pattern occurs when $R = 1$, if the R index approaches zero the pattern is aggregate and when R index has a maximum limit around 2.15 the pattern is regular. The z value was calculated to determine whether the observed distribution was significantly different from the expected random pattern (Klimas et al., 2007). The K function was determined by the Splancs package (Rowlingson & Diggle, 2017) and the aggregation index R by the Spatstat package (Baddeley & Turner, 2005), both from the R software (R core Team, 2019).

2.3.2 | Age and growth patterns

Tree age was determined by quantifying the growth ring structures formed by marginal parenchyma (Figure 2; Fichtler et al., 2003). For hollow trees (two trees), the missing rings were estimated by the mean number of rings of the other samples (Brienen & Zuidema, 2006).

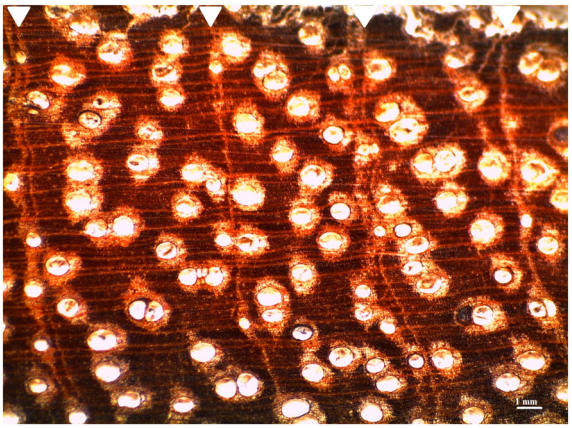

FIGURE 2 Anatomical structure of the growth rings, formed by bands of marginal parenchyma, of *Pentaclethra macroloba* in the Amazon estuary [Color figure can be viewed at wileyonlinelibrary.com]

The structures were visualized and quantified using a stereomicroscope with an attached camera.

The current radial increment (based on the width of the growth rings) was adjusted to the field diameter to construct the cumulative diametric growth curve for each individual (Brienen & Zuidema, 2006). The cumulative curve of each individual was used to obtain the mean diametric growth curve, which was adjusted to the sigmoid regression model (Equation 7) as proposed by Schöngart et al. (2007). The relationship between the height and diameter of each individual was assessed and adapted using the nonlinear regression model (Equation 8; Schöngart, 2008).

$$\text{dbh} = \frac{a}{\left[1 + \left(\frac{b}{\text{age}}\right)^c\right]}, \tag{7}$$

$$H = \text{dbh} \times d/\text{dbh} + e, \tag{8}$$

a, b, c, d, and e are estimated parameters of the model.

The rates of current annual increment (CAI; Equation 9) and mean annual increment (MAI; Equation 10) of diameter, height and biomass were derived for the corresponding age of each individual (Schöngart et al., 2007). To estimate aboveground biomass (Equation 11) we used the pantropical allometric equation, proposed by Chave et al. (2014).

$$\text{CAI} = \text{CG}_{(t+1)} - \text{CG}_{(t)}, \tag{9}$$

$$\text{MAI} = \frac{\text{CG}_{(t)}}{t}, \tag{10}$$

$$Biomass_t = 0.0673 \times \left(H_t \times \text{dbh}_t^2 \times \rho\right)^{0.976}, \tag{11}$$

CG = accumulated growth in different years t throughout the species lifespan; and ρ = wood density. For *P. macroloba* the wood density is 0.65 g/cm^3 (Reyes et al., 1992).

The successional trajectory of *P. macroloba* in the forest canopy was evaluated using the patterns of release and suppression that occurred throughout its history of growth over time. These patterns were detected from the series of widths of the growth rings of each individual, and interpreted by the expression proposed by Nowacki and Abrams (1997):

$$\%GC_i = \left[\frac{M2 - M1}{M1}\right] \times 100, \quad (12)$$

$\%GC_i$ = percentage of growth change in the preceding 10 years and subsequent 10 years; $M1$ = mean diametric growth of preceding 10 years; and $M2$ = mean diametric growth of subsequent 10 years.

Release events occur when relative growth is above 100% for five consecutive years and suppression events occur when relative growth is below −50% for five consecutive years (Brienen et al., 2010). The growth trajectory in diameter of the species was classified into four patterns: (1) direct growth: occurs when the tree has no release or suppression events; (2) one release event: when the tree shows an increase in relative growth for five consecutive years; (3) one suppression event: when the tree shows a decrease in relative growth for five consecutive years; and (4) multiple release and suppression events: when two or more release and suppression events occur (Nowacki & Abrams, 1997; Schöngart et al., 2015).

The relationship between the diametric growth of *P. macroloba* and the hydroclimatic variables (temperature, rainfall and flood level in high and low floodplain environments) was evaluated using multiple regressions (Schöngart et al., 2002) and the statistical differences between the two environments were evaluated by the ANOVA test (Dantas et al., 2020).

3 | RESULTS

3.1 | Population structure of adult trees

Two thousand and seventy-two individuals were censured, that is, a population density of 15 individuals

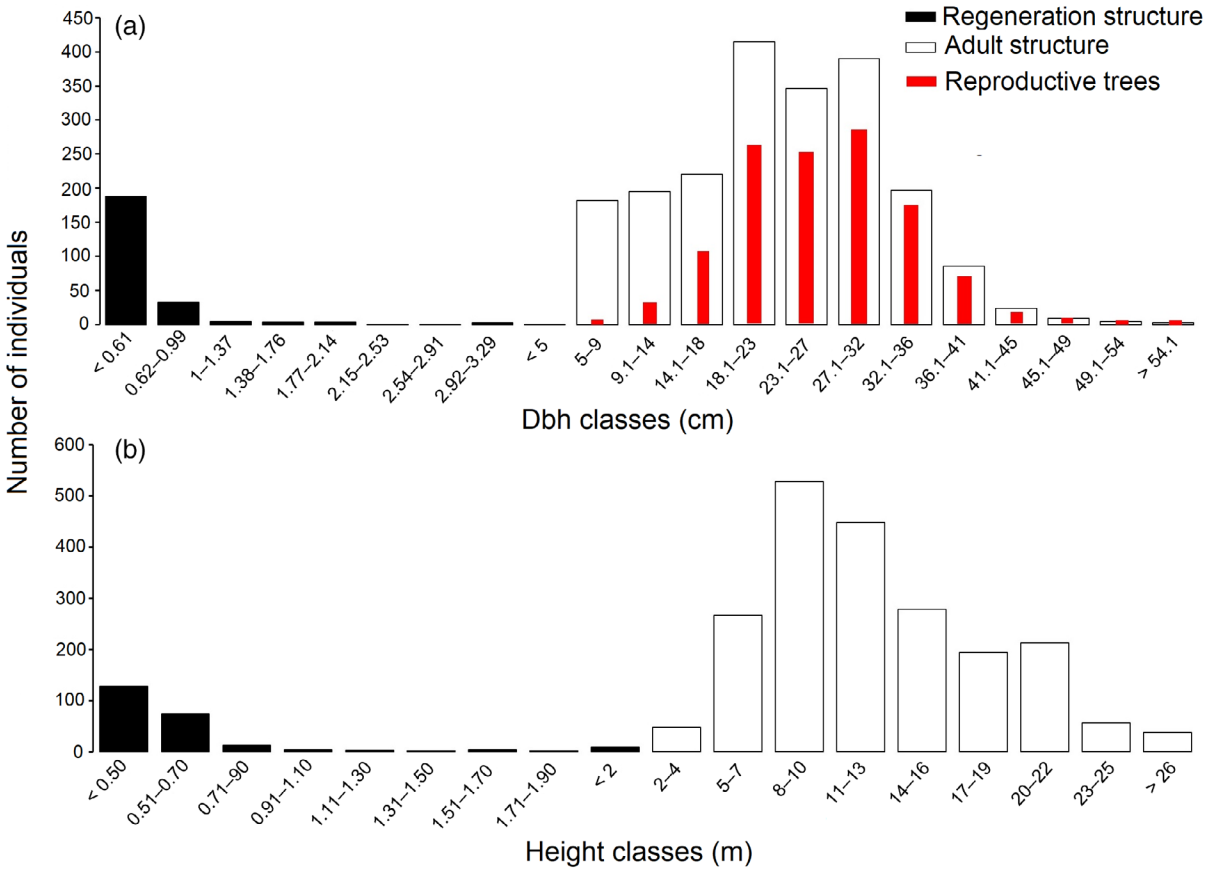

FIGURE 3 Diameter (a) and height (b) distribution pattern of the regeneration (seedlings and saplings) and adult trees of a population of *Pentaclethra macroloba* in the Amazon estuary [Color figure can be viewed at wileyonlinelibrary.com]

ha^{-1}. The population was distributed into 12 diameter classes, with 4 cm of interclass amplitude and mean dbh of 23 cm (±9 cm). The central classes, which have diameters between 18.1 and 32 cm, had greater population density (9 individuals ha^{-1}) than the first (diameters from 5 to 18 cm with 4 individuals ha^{-1}) and the last classes (diameters >32.1 cm with 2 individuals ha^{-1}), approximated by a log-normal distribution (Figure 3a).

The total basal area of the *P. macroloba* population was 98.13 m^2 (total basal area of 2072 trees sampled in 136.59 ha), equivalent to 0.72 m^2 ha^{-1}, with a mean of 0.048 m^2 (±0.035 m^2) per tree. The diameter classes from 18.1 to 41 cm were those that most concentrated basal area (85.80 m^2), representing 86% of the total basal area.

The majority of the *P. macroloba* population consisted of reproductive trees. In total, 1235 trees (59% of the population) had some reproductive characteristics, such as flowers and fruits or traces of both. Minimum and maximum reproductive dbh were 7 and 70 cm, respectively, with a mean of 26 cm (±7 cm). Most reproductive trees (79%) were concentrated between the dbh from 18.1 to 36 cm (Figure 3a, red bars).

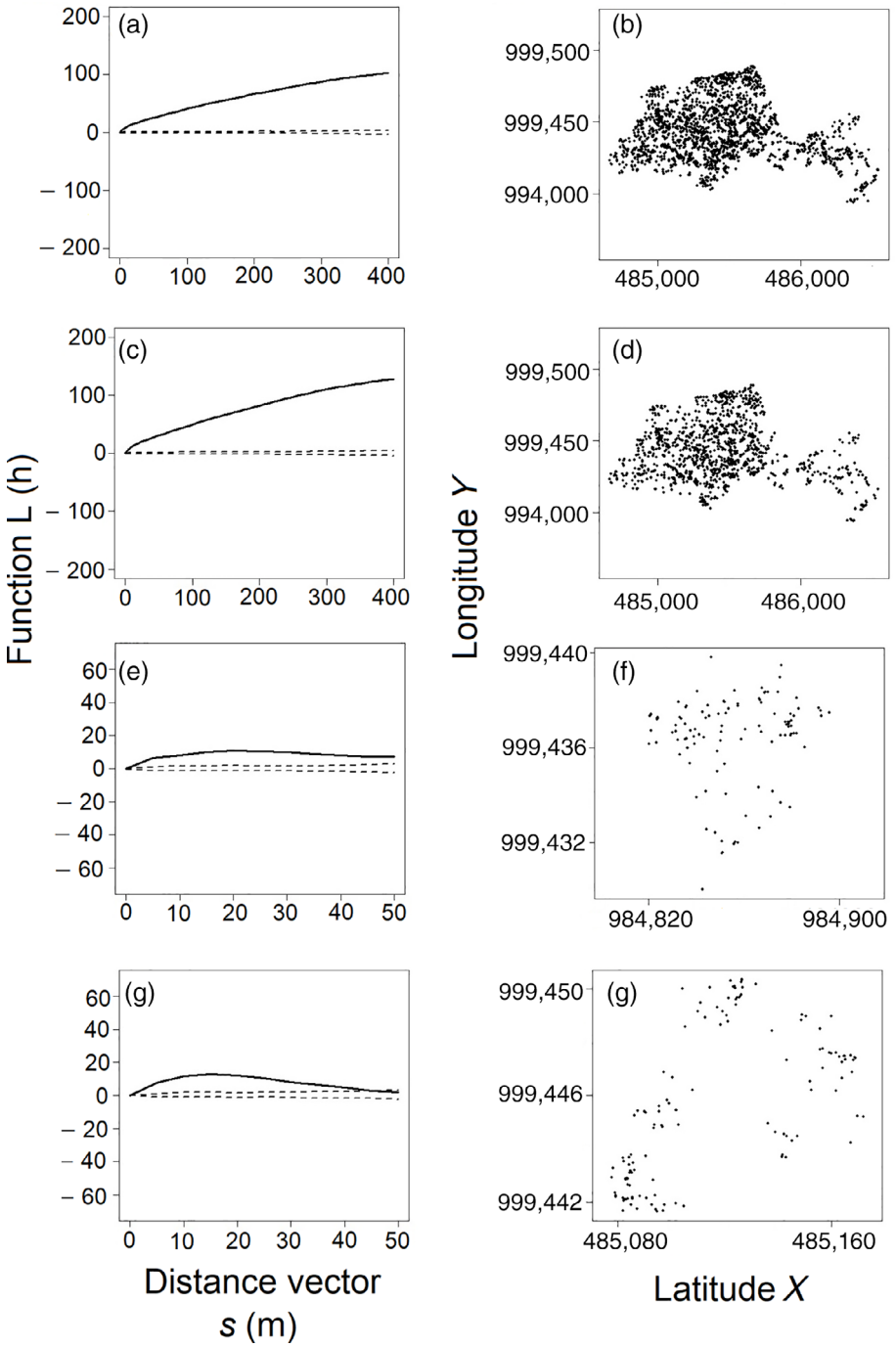

FIGURE 4 Spatial distribution pattern of adult trees (population [a, b] and reproductive individuals [c, d]) and regeneration (plot 1 [e, f] and plot 2 [g, h]) of a population of *Pentaclethra macroloba* in the Amazon estuary. Solid line is the function *K* transformed into function *L*, dashed lines are the confidence envelopes and dots are the individuals of *Pentaclethra macroloba*

In the forest canopy, most *P. macroloba* individuals were classified as codominant (61%), followed by dominant (25%), and suppressed (14%). The population had a mean height of 12.7 m (±5.4 m) and the distribution pattern was similar to the diameter (Figure 3b).

The population of *P. macroloba* also presented a spatially aggregated pattern in all distance scales of the vector *s(m)* (Figure 4a), being evidenced by an aggregation index <1 ($R = 0.63$; $p < 0.002$) and as shown in the distribution map (Figure 4b). The mean distance between neighboring trees was 8.5 m (±6.4 m), with minimum and maximum of 0.26 and 54.5 m, respectively. Reproductive individuals also presented an aggregated pattern at all geographical distances (Figure 4c), with aggregation index $R = 0.62$ ($p < 0.002$). The mean distance of a reproductive individual to another was 10.8 m (±8.3 m), with minimum and maximum distances of 0.33 and 75.4 m, respectively.

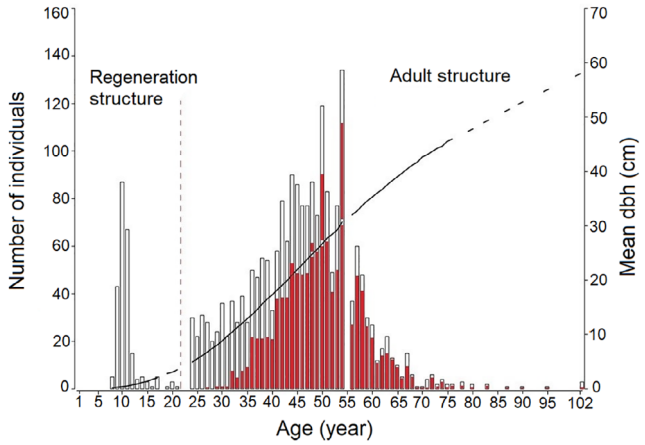

FIGURE 5 Age structure of regeneration (seedlings and saplings) and adult trees (reproductive trees red bars) of a population of *Pentaclethra macroloba* in the Amazon estuary [Color figure can be viewed at wileyonlinelibrary.com]

3.2 | Population structure of the regeneration

Tree regeneration consisted of 240 individuals, a density of 120 individuals ha^{-1} (226 seedlings and 14 saplings). *Pentaclethra macroloba* regeneration was distributed in eight diametric classes, with an amplitude of 0.38 cm between classes and mean diameter of 0.62 cm (±0.48 cm). The diametric distribution pattern of regeneration was exponential, 92% of individuals with dbh < 0.99 cm (Figure 3a).

The mean height of the regenerants was 0.63 m (±0.55 m), with minimum and maximum height 0.16 and 4.9 m, respectively. Most individuals had a height < 0.70 m, showing exponential distribution pattern (Figure 3b).

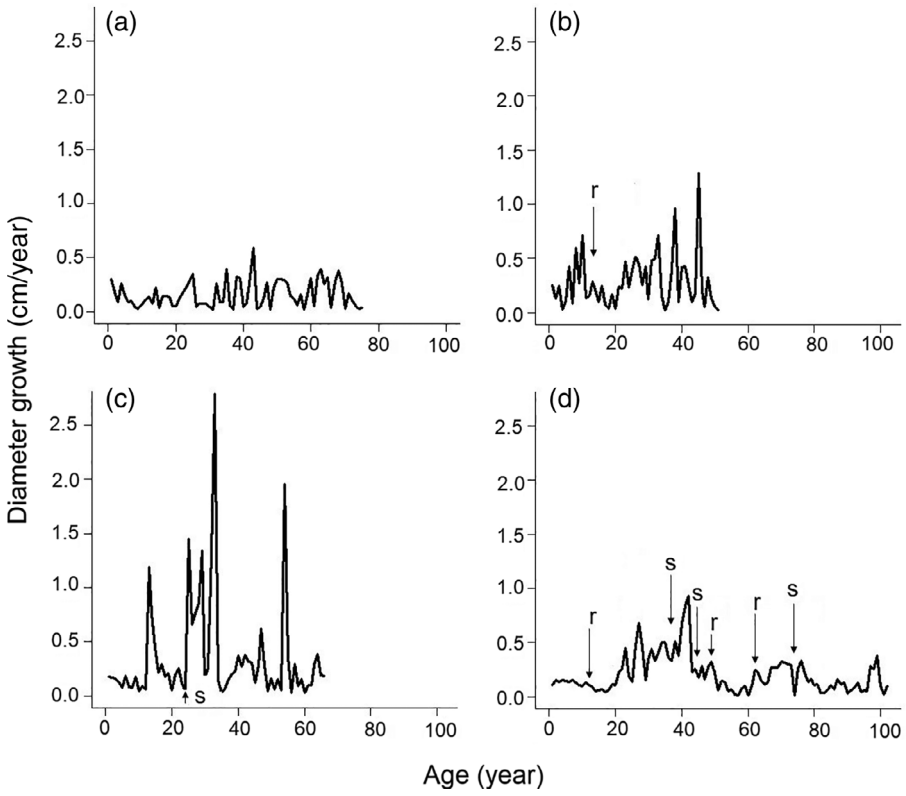

FIGURE 6 Growth patterns of *Pentaclethra macroloba* during its life trajectory in the Amazon estuary: (a) direct growth, (b) one release, (c) one suppression and (d) multiple events of release and suppression. Release (r) and suppression (s)

Aggregate distribution patterns predominated, mainly in plot one (Figure 4e,f). In plot two, there was randomness in the scales from 46 to 50 m (Figure 4g). Despite this, the *R* index showed strong aggregation for plots one ($R = 0.54$; $p < 0.002$) and two ($R = 0.51$; $p < 0.002$). The mean distance between regenerants found for plots one and two were 2.7 m (±2.7 m) and 2.3 m (±2.4 m), respectively.

3.3 | Age and growth pattern

The mean age of the 38 sampled individuals of *P. macroloba* was 60 years (±20 years), with a minimum and maximum age of 28 and 102 years, respectively. With the growth models it was possible to estimate the age for both regenerating and adult trees (Figure 5). The mean age of the 240 seedlings and saplings, with dbh ranging from 0.22 cm to 3.55 cm, was 11 years (±2 years), with a minimum and maximum age of 8 years and 21 years, respectively. For the 2072 adult trees with dbh > 5 cm, the mean age was 46 years (±11 years), with a minimum and maximum of 24 and 102 years, respectively. Estimates indicated that *P. macroloba* reproductive maturity is around 27 years old, with a 7 cm dbh (Figure 5, red bars). The mean age of the sampled reproductive trees was 42 years (±10 years) and the maximum was 102 years.

During the life trajectory of *P. macroloba*, in search of the forest canopy, the species grown freely (Figure 6a) and presented release (Figure 6b), suppression (Figure 6c) and multiple release and suppression events (Figure 6d). Most of the trees showed direct growth (15 events = 47%), not manifesting liberation or suppression events. Eight release events (25%), seven suppression events (22%) and two multiple release and suppression events (6%) were recorded.

From the 1988 measured growth rings, the mean ring width was 3.1 mm year^{-1} (±1.3 mm year^{-1}). The relationship between age and diameter of *P. macroloba* was highly significant ($r^2 = 0.98$; $p < 0.001$), allowing the modeling of the accumulated diametric growth curve of the individuals (Figure 7a). A significant relationship was also found for height and diameter ($r^2 = 0.79$; $p < 0.001$; Figure 7b). The peak of diameter increment of *P. macroloba* occurred at the age of 46 years (9.38 mm year^{-1}),

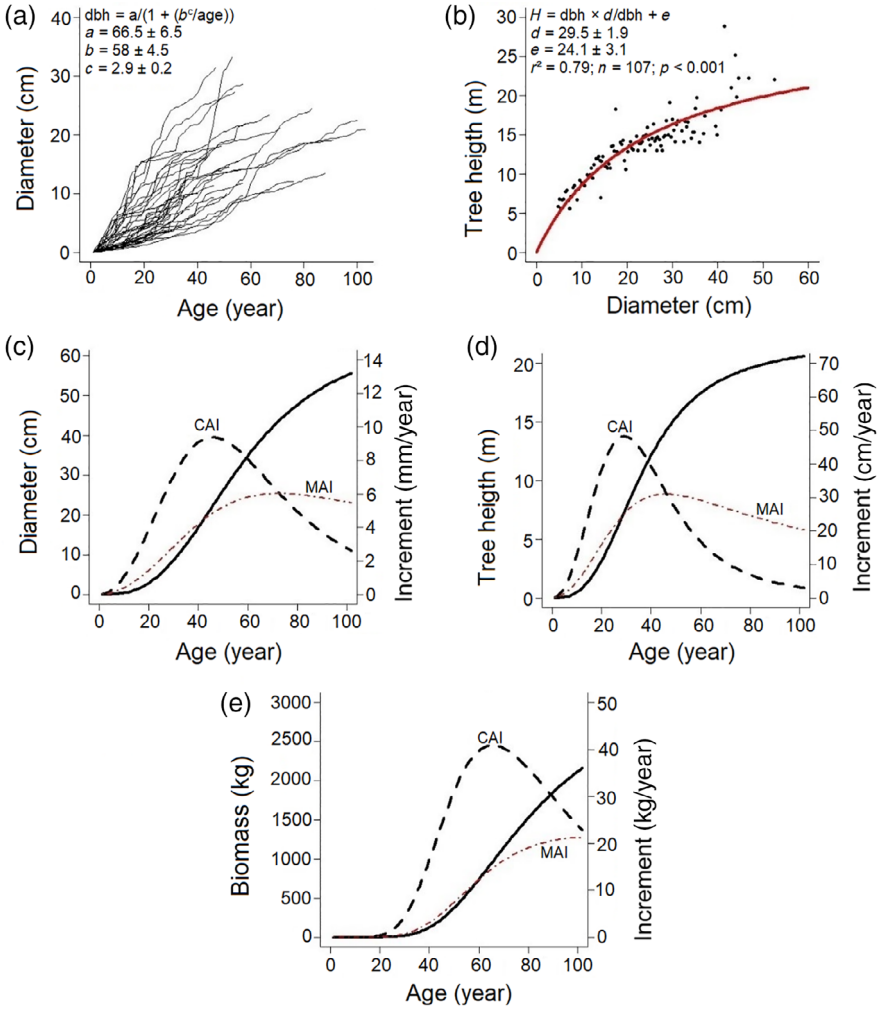

FIGURE 7 Growth patterns and biomass stock of *Pentaclethra macroloba* during its life trajectory in the Amazon estuary: Accumulated diameter (a), relationship between height and diameter (b); and increment in diameter (c), height (d) and biomass (e). Current annual increment (CAI) and mean annual increment (MAI) [Color figure can be viewed at wileyonlinelibrary.com]

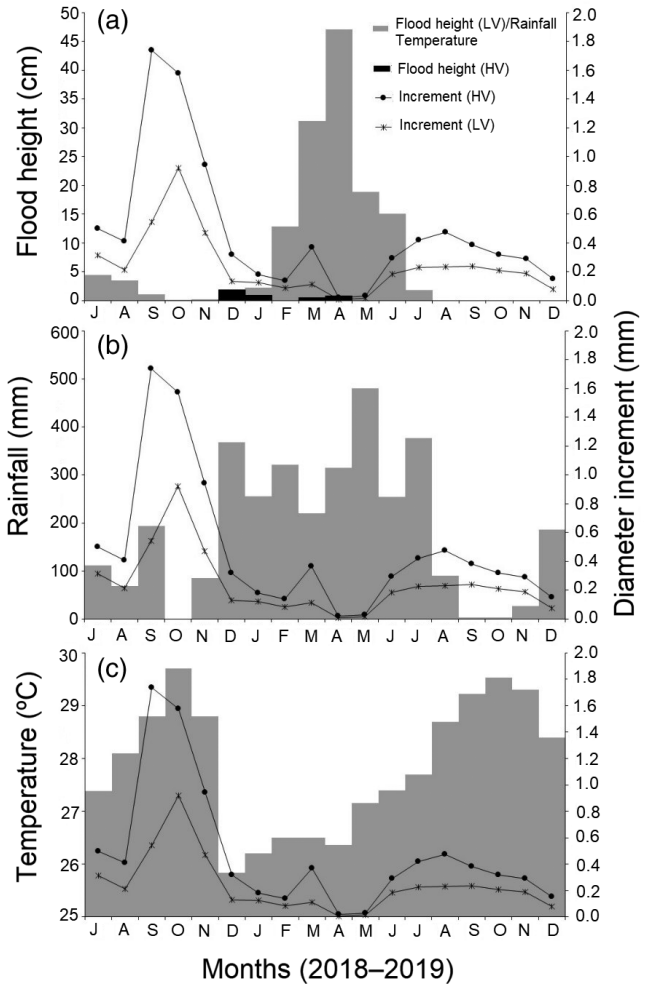

FIGURE 8 Relationships between flood level in the interior of the forest (a), monthly rainfall (b) and mean monthly maximum temperature (c) with the diametric increment of *Pentaclethra macroloba* in high floodplain (HV) and low floodplain (LV) in the Amazon estuary

when the species had 22 cm of dbh (Figure 5c). The peak height increment occurred at the age of 24 years (61.7 cm $year^{-1}$), well before of the peak of diametric increment, when height and dbh corresponded to 7.3 m and 8 cm, respectively (Figure 7d). The peak of increment in biomass occurred at the age of 66 years (40.8 kg $year^{-1}$), when the total biomass corresponded to 982.3 kg and when the species reached dbh of 39 cm and height of 18 m (Figure 7e).

3.4 | Influence of the hydrometeorological variables in the diametric growth

The mean diametric increment of high floodplain trees was slightly greater (0.25 mm ± 0.56 mm) than the low floodplain trees (0.24 mm ± 0.61 mm), but without statistical significance ($F = 0.001$; $p = 0.97$). The mean level of flooding between the two environments differed statistically ($F = 6$; $p < 0.01$), with low floodplain trees experiencing greater flooding amplitudes (7.81 cm ± 13.08 cm), compared with the trees of the high floodplain (0.25 cm ± 0.54 cm).

The trees in both environments showed greater diametric increment during the dry season (from September to December) when the tides of the Amazon River do not reach the forest soil (Figure 8a) due to a decrease in the rainfall (Figure 8b) and the increase of the temperature (Figure 8c). In the rainy season (Figure 8b) with the highest levels of flooding (this period corresponds from January to July, with greater intensity from March to April), the diametric increment of the species decreased. The peak diametric increments were recorded in the high and low floodplain in September (1.2 mm) and October (0.92 mm) of 2018, respectively. The diametric increment of the low floodplain trees had a significant and negative correlation with flooding ($R^2 = 0.47$; $t = -3.01$; $p < 0.01$) and rainfall ($R^2 = 0.41$; $t = -2.62$; $p < 0.01$). The correlation of diametric increment was also significant and positive with the maximum temperature ($R^2 = 0.44$; $t = 2.81$; $p = < 0.05$). In the high floodplain, the diametric increment of the trees also correlated negatively with the flood height and rainfall, and positively with the maximum temperature, but there was no statistical significance.

4 | DISCUSSION

A greater stock of seedlings in the understory and higher density of trees in the central diameter classes are structural features of late secondary species, ecological group according to the Budowski classification (Budowski, 1970). *Pentaclethra macroloba* would then belong to this group that shows a discontinuity in recruiting individuals over time (Peters, 1996) and depends on large disturbances to establish in the forest canopy. *Pentaclethra macroloba* seedlings appear to be adapted to the low light of the understory and they persist for a long time suppressed below the forest canopy (up to 11 years in the understory Figure 5), waiting for openings to reach the canopy (Oberbauer & Strain, 1985). In the *La Selva* Forest Reserve, Costa Rica, *P. macroloba* is gap colonist and it was shown to depend on canopy gaps to reach the forest canopy (Brandani et al., 1988). The pattern of diametric distribution here corroborates other studies in different parts of the Amazon estuary (Dantas et al., 2017) and in Central America where *P. macroloba* is monodominant (Galván et al., 2003).

Although the adult trees present a log-normal distribution pattern, the natural regeneration shows a very stable and auto-regenerative structure, with its inverted "J" distribution pattern (Miranda et al., 2018). This characteristic is important, as the regenerants provide for a constant flow of trees to the upper classes.

Flood dynamics and climatic seasonality of the estuarine floodplain forest are factors that shape the population structure of *P. macroloba*. The estuarine floodplain soils are fragile, due to daily tides that deposit and remove sediments from the forest, causing erosion. According to Metzger et al. (1997), this makes the rhizosphere unstable, directly affecting seedling development and the stability of adult trees. The dry season of the estuary (from September to December) also affects the rate of recruitment. During this period, seedlings experience a prolonged water stress, because the flood does not reach the interior of the forest due to decreased rainfall. In a seasonally flooded forest in Darien, Panama, Lopez and Kursar (2007) found that the seedling mortality rate of *P. macroloba* was higher in the dry season (43%) than in the rainy season (9.4%). These environmental conditions regulate the dominance of *P. macroloba* and maintain the population growth rate stable. Seedlings that can better adapt to environmental conditions are the few that will grow past the last size classes of the regeneration structure.

Many of the aggregate patterns found in tropical trees may be related to dispersal limitation (Condit et al., 2000) and to environmental factors of the habitat (Dantas et al., 2017). When individuals of *P. macroloba* disperse their seeds by the explosive dehiscence of the fruits (primary dispersal by autochory), they launch their propagules at a distance of approximately 10 m (Hartshorn, 1983), allowing them to be subsequently transported by the river flow (secondary dispersal by hydrochory). The outflow and inflow of the daily river tide facilitates the exit and entry of forest seeds (Cunha et al., 2017). Groups of seeds can be transported over long distances or remain close to the mother tree, as many are intercepted by branches and trunks present on the forest floor (Ziburski, 1991). The result is that few seeds germinate alone, resulting in an aggregated pattern of regeneration. The trees of the Amazon estuary synchronize the phase of seed dispersal with the peak river flood (Cattanio et al., 2004; Dantas et al., 2016). This strategy facilitates the reproductive success of the mother tree and the establishment of new seedling groups in the floodplain soil.

We found centennial trees of *P. macroloba* (maximum age of 102 years) inhabiting the Amazon estuary, showing that *P. macroloba* is a long-lived late secondary species and is tolerant to the daily tidal of the Amazon River. This tolerance to flooding of the Amazon estuary can be attributed to the adaptation mechanisms that *P. macroloba* has developed to tolerate the anoxic rhizosphere, such as: numerous protruding lenticels on the tree trunk which facilitate the transport of oxygen to the root and to the aerial parts of the plant, and adventitious roots which increase the respiratory efficiency of the root (Dantas, Guedes, Vasconcelos, et al., 2021). In Central America, populations of *P. macroloba* were also long-lived. In a study carried out in the *La Selva* forest, Costa Rica, Lieberman et al. (1985) conducted successive measurements on trees during 13 years, the first measurement in 1969 and the last in 1982, and based on the dbh measurements, the authors projected the life span of *P. macroloba* to 312 years.

The sigmoid growth pattern over time for *P. macroloba* (Figure 5) shows different periods of its life trajectory and the degree of conservation of the forest. According to Köhl et al. (2017), the sigmoid growth curve reveals three phases: pre-reproductive, maturity and senescence. Possibly, the log-normal pattern of the diameter distribution of *P. macroloba* reflects these three phases (comparison of Figures 3a and 7c). Classes from 5 to 18 cm in diameter belong to pre-reproductive individuals, representing 28.8% of the population and are on the increasing curve of the diametric increment. The classes from 18.1 to 32 cm belong to mature individuals, represent 55.6% of the population and are at the peak of diametric increment. The classes >32.1 cm belong to senescent trees, they represent 15.6% of the population, and they are on the decreasing curve of the diametric increment dominating the biomass stocks. Over the time of the plant development, the production rate of woody material of the tree increases, by the increase in photosynthetic rate, due to expansion of the leaf and crown area (Sillett et al., 2010). This confirms the ecological relevance of old trees as carbon reservoirs (Köhl et al., 2017).

Different growth patterns were observed during the life cycle of *P. macroloba* in the conquest of the forest canopy (Figure 4). Most of the trees studied showed direct growth, followed by release events. This pattern reinforces the idea that *P. macroloba* depends on gaps to stimulate natural regeneration (Valverde-Barrantes & Rocha, 2014). The seed groups that are intercepted by fallen tree branches in the gaps germinate and grow freely toward the canopy because, in these conditions, no physical barriers shed light. Competition for light stimulates a faster increment in height than in diameter for the predominance of codominant trees in the canopy (61% of trees). For Brienen and Zuidema (2006), trees that do not experience events of release or suppression during succession, probably experience very stable light conditions,

or the light fluctuations are less limiting for individuals, allowing them to grow toward the canopy in less time. Multiple events of release and suppression at different times during the life history of the tree, evidence that the forest canopy opened and closed several times due to formation of gaps or damage in the tree crown, causing increase and decrease of growth, respectively (Brienen & Zuidema, 2006).

In Costa Rica, *P. macroloba* trees that are codominant or dominant in the canopy, and thus are more exposed to sunlight, show more significant diametric increment than trees suppressed by the crown of neighboring trees (Galván et al., 2003). The dependence of growth canopy gaps becomes clear when *P. macroloba* is subjected to silvicultural release techniques followed by refinement (elimination of neighboring trees and undesirable species). Individuals of the species subjected to silvicultural release show rapid diametric increment (6 mm $year^{-1}$), compared to individuals who receive a few silvicultural interventions (3 mm $year^{-1}$; Finegan et al., 1999).

Although the general pattern of trees growth is to first grow in height and then in diameter, as observed in *P. macroloba* (comparison of Figure 5b,c), in periodically flooded forests, this strategy is also essential for the plant to escape the flooding in its early stages of life (Parolin, 2002). According to Newbery and Ridsdale (2016), understory trees have a strategy of concentrating more resources into height growth, as they seek the forest canopy to increase the photosynthetic rate and decrease competition for light, and only subsequently to invest into diameter increment. This type of strategy was also observed by Miranda et al. (2018) for the estuarine species *Mo. paraensis*.

The existence of growth rings for *P. macroloba* is an important discovery for the floodplains of the Amazonian estuary. Until the present study, only the existence of annual rings for *Mo. paraensis* was confirmed (Miranda et al., 2018). The annual rings that form on the tree trunk of flooded Amazonian forests can be associated with the seasonality of this habitat. We showed that the seasonal rainfall of the Amazonian estuary and the increase in the level of flooding of the Amazon River regulate the growth rate of *P. macroloba* and cause physiological stress on the cambial activity of the species. This is strong evidence that these two seasonal phenomena is the cause for the formation of the annual rings of *P. macroloba* in the Amazon estuary. In the floodplain forest of the Central Amazon, Schöngart et al. (2005) also found a high association between the seasonal flood pulse of these forests with the width of the growth rings of *Macrolobium acaciifolium*.

The high rainfall at the mouth of the Amazon River during the rainy season, raise the level of the river (Cunha et al., 2017) and its tributaries, resulting in daily flooding inside the forest. Seasonal increase in water levels from flooding causes the stagnation of cambial activity in *P. macroloba* (Figure 8), especially in the low floodplain individuals who are more exposed to flooding. According to Worbes and Fichtler (2010), the flooded soil promotes rhizosphere anoxicity, impairing the roots breath and upward water transport to the tree crown. The cambial growth of *P. macroloba* is resumed in the dry season, when the flood does not reach the interior of the forest, due to the decrease in the volume of rainfall in the region. This phenomenon is similar to what occurs with trees in the Central Amazon, where they experience a long-term and high-amplitude flood regime (Schöngart et al., 2002). Trees have a greater diameter increment in the terrestrial phase (river level retreat) because in the aquatic phase, floods cause a cambial dormancy (Schöngart et al., 2002). In the tropical rainforest of *La Selva* in Costa Rica, in periodically flooded forests, *P. macroloba* also had the greatest diameter increment (1.06 cm $year^{-1}$) during the dry season, from December to April (Hazlett, 1987).

The demographic and growth patterns of *P. macroloba* respond to the environmental heterogeneity of the estuarine floodplain forest and also reflect its life history. Increases in rainfall and flood level of the Amazon River in the rainy season regulate the growth rate of *P. macroloba*, making it a seasonal process. Long years tolerating the daily flooding of the Amazon River made *P. macroloba* a hyperdominant tree highly specialized in colonizing the floodplains of the Amazon estuary. Natural gaps and the incidence of light keep the growth rate of *P. macroloba* high. We have elucidated some important gaps of the scientific knowledge about the natural history of *P. macroloba* populations of the Amazon basin, particularly in the estuarine floodplain region. In this way, we provide foundational knowledge for the formulation of public policies for the sustainable management and conservation of natural resources of *P. macroloba* and its multiple uses.

ACKNOWLEDGMENTS

We thank the Programa de Pós-graduação em Ecologia (INPA/PPGEco), Instituto Nacional de Pesquisas da Amazônia (INPA), Empresa Brasileira de Pesquisa Agropecuária (Embrapa Amapá), Grupo Ecologia, Monitoramento e Uso Sustentável de Áreas Úmidas (MAUA/PELD/CNPq/FAPEAM) and field technicians from Embrapa Amapá: Paulo, Adijalma, Enoque, and Jonas.

CONFLICT OF INTEREST

The authors declare that they have no conflict of interest.

AUTHOR CONTRIBUTIONS

Adelson Rocha Dantas: Investigation; conceptualization; methodology; formal analysis; visualization; writing—original draft. **Marcelino Carneiro Guedes**: Writing—review and editing; conceptualization; supervision. **Ana Cláudia Lira-Guedes**: Writing—review and editing; conceptualization; project administration; Funding acquisition. **Jochen Schöngart**: Conceptualization; methodology; formal analysis; writing—review and editing. **Maria Teresa Fernandez Piedade**: Writing—review and editing; conceptualization; supervision.

ORCID

Adelson Rocha Dantas https://orcid.org/0000-0001-6213-5953

REFERENCES

Alvares, C. A., Stape, J. L., Sentelhas, P. C., de Gonçalves, J. L. M., & Sparovek, G. (2014). Köppen's climate classification map for Brazil. *Meteorologische Zeitschrift*, *22*(6), 711–728. https://doi.org/10.1127/0941-2948/2013/0507

Baddeley, A., & Turner, R. (2005). spatstat: An R package for analyzing spatial point patterns. *Journal of Statistical Software*, *12*(6), 3–4. https://doi.org/10.18637/jss.v012.i06

Banov, D., Banov, F., & Bassani, A. S. (2014). Case series: The effectiveness of fatty acids from pracaxi oil in a topical silicone base for scar and wound therapy. *Dermatology and Therapy*, *4*(2), 259–269. https://doi.org/10.1007/s13555-014-0065-y

Brandani, A., Hartshorn, G. S., & Orians, G. H. (1988). Internal heterogeneity of gaps and species richness in Costa Rican tropical wet forest. *Journal of Tropical Ecology*, *4*(2), 99–119. https://doi.org/10.1017/S0266467400002625

Brienen, R. J. W., & Zuidema, P. A. (2006). Lifetime growth patterns and ages of Bolivian rain forest trees obtained by tree ring analysis. *Journal of Ecology*, *94*(2), 481–493. https://doi.org/10.1111/j.1365-2745.2005.01080.x

Brienen, R. J. W., Zuidema, P. A., & Martínez-Ramos, M. (2010). Attaining the canopy in dry and moist tropical forests: Strong differences in tree growth trajectories reflect variation in growing conditions. *Oecologia*, *163*(2), 485–496. https://doi.org/10.1007/s00442-009-1540-5

Budowski, G. (1970). The distinction between old secondary and climax species in tropical central American lowlands. *Tropical Ecology*, *11*(1), 44–48.

Carim, M. J. V., Wittmann, F. K., Piedade, M. T. F., Guimarães, J. R. S., & Tostes, L. C. L. (2016). Composition, diversity, and structure of tidal "Várzea" and "Igapó" floodplain forests in eastern Amazonia, Brazil. *Brazilian Journal of Botany*, *40*(1), 115–124. https://doi.org/10.1007/s40415-016-0315-6

Cattanio, J. H., Anderson, A. B., Rombold, J. S., & Nepstad, D. C. (2004). Phenology, litterfall, growth, and root biomass in a tidal floodplain forest in the Amazon estuary. *Revista Brasileira de Botânica*, *27*(4), 703–712. https://doi.org/10.1590/S0100-84042004000400010

Chave, J., Réjou-Méchain, M., Búrquez, A., Chidumayo, E., Colgan, M. S., Delitti, W. B. C., Duque, A., Eid, T., Fearnside, P. M., Goodman, R. C., Henry, M., Martínez-Yrízar, A., Mugasha, W. A., Muller-Landau, H. C., Mencuccini, M., Nelson, B. W., Ngomanda, A., Nogueira, E. M., Ortiz-Malavassi, E., … Vieilledent, G. (2014). Improved allometric models to estimate the aboveground biomass of tropical trees. *Global Change Biology*, *20*(10), 3177–3190. https://doi.org/10.1111/gcb.12629

Clark, P. J., & Evans, F. C. (1954). Distance to nearest neighbor as a measure of spatial relationships in populations. *Ecology*, *35*(4), 445–453. https://doi.org/10.2307/1931034

Condit, R., Ashton, P., & Baker, P. (2000). Spatial patterns in the distribution of tropical tree species. *Science*, *288*(May), 1414–1418. https://doi.org/10.1126/science.288.5470.1414

Costa, M. N. F. S., Muniz, M. A. P., Negrão, C. A. B., da Costa, C. E. F., Lamarão, M. L. N., Morais, L., Morais, L., Júnior, J. O. C. S., & Ribeiro Costa, R. M. (2014). Characterization of *Pentaclethra macroloba* oil. *Journal of Thermal Analysis and Calorimetry*, *115*(3), 2269–2275. https://doi.org/10.1007/s10973-012-2896-z

Cunha, A. C., Mustin, K., dos Santos, E. S., dos Santos, É. W. G., Guedes, M. C., Cunha, H. F. A., Rosman, P. C. C., & da Sternberg, L. S. L. (2017). Hydrodynamics and seed dispersal in the lower Amazon. *Freshwater Biology*, *62*(10), 1–9. https://doi.org/10.1111/fwb.12982

da Silva, J. O., Fernandes, R. S., Ticli, F. K., Oliveira, C. Z., Mazzi, M. V., Franco, J. J., Giuliatti, S., Pereira, P. S., Soares, A. M., & Sampaio, S. V. (2007). Triterpenoid saponins, new metalloprotease snake venom inhibitors isolated from *Pentaclethra macroloba*. *Toxicon*, *50*(2), 283–291. https://doi.org/10.1016/j.toxicon.2007.03.024

Dantas, A. R., Guedes, M. C., Lira-Guedes, A. C., & Piedade, M. T. F. (2021). Phenological behavior and floral visitors of *Pentaclethra macroloba*, a hyperdominant tree in the Brazilian Amazon River estuary. *Trees—Structure and Function*, *35*(3), 973–986. https://doi.org/10.1007/s00468-021-02095-x

Dantas, A. R., Guedes, M. C., Vasconcelos, C. C., Isacksson, J. G. L., Pastana, D. N. B., Lira-guedes, A. C., & Piedade, M. T. F. (2021). Morphology, germination, and geographic distribution of *Pentaclethra macroloba* (Fabaceae): A hyperdominant Amazonian tree. *Revista de Biología Tropical*, *69*(1), 181–196. https://doi.org/10.15517/rbt.v69i1.43446

Dantas, A. R., Lira-Guedes, A. C., Guedes, M. C., Piedade, M. T. F., & Batista, A. P. (2020). Population dynamics of *Attalea excelsa* (Arecaceae) in floodplain forest of the amazonian estuary. *Journal of Tropical Forest Science*, *32*(2), 105–113. https://doi.org/10.26525/jtfs32.2.105

Dantas, A. R., Lira-Guedes, A. C., Mustin, K., Aparício, W. C. S., & Guedes, M. C. (2016). Phenology of the multi-use tree species *Carapa guianensis* in a floodplain forest of the Amazon estuary. *Acta Botanica Brasilica*, *30*(4), 618–627. https://doi.org/10.1590/0102-33062016abb0282

Dantas, A. R., Marangon, L. C., Guedes, M. C., Feliciano, A. L. P., & Lira-Guedes, A. C. (2017). Spatial distribution of a population of *Pentaclethra macroloba* (Willd.) Kuntze in a floodplain forest of the Amazon estuary. *Revista Árvore*, *41*(4), 1–11. https://doi.org/10.1590/1806-90882017000400006

Dawkins, H. C. (1958). *The management of natural tropical high-forest with special reference to Uganda*. University of Oxford/Imperial Forestry Institute.

de Vilhena, J. E. S., Lima e Silva, R. B., & da Freitas, J. L. (2018). *Climatologia do Amapá: quase um século de história*. Gramma.

Ferreira, L. V., & Stohlgren, T. J. (1999). Effects of river level fluctuation on plant species richness, diversity, and distribution in a floodplain forest in Central Amazonia. *Oecologia*, *120*(4), 582–587. https://doi.org/10.1007/s004420050893

Fichtler, E., Clark, D. A., & Worbes, M. (2003). Age and long-term growth of trees in an old-growth tropical rain Forest, based on analyses of tree rings and $^{14}C^{1}$. *Biotropica*, *35*(3), 306–317. https://doi.org/10.1111/j.1744-7429.2003.tb00585.x

Finegan, B., Camacho, M., & Zamora, N. (1999). Diameter increment patterns among 106 tree species in a logged and silviculturally treated Costa Rican rain forest. *Forest Ecology and Management*, *121*(3), 159–176. https://doi.org/10.1016/S0378-1127(98)00551-9

Galván, O., Louman, B., Galloway, G., & Obando, G. (2003). Efecto de la iluminación de la copa sobre el crecimiento de *Pentaclethra macroloba* y *Goethalsia meiantha* e implicaciones para la silvicultura de los bosques tropicales húmedos. *Recursos Naturales y Ambiente*, *46*, 117–126.

Goreaud, F., Courbaud, B., & Collinet, F. (1997). Spatial structure analysis applied to modelling of forest dynamics: A few examples. *Proceedings of the IUFRO Workshop, Empirical and Process Based Models for Forest Tree and Stand Growth Simulation*, *21*, 27–1055. https://doi.org/10.1111/ecog.01579

Hartshorn, G. S. (1983). *Pentaclethra macroloba* (Gavilan). In D. H. Janzen (Ed.), *Costa Rican natural history* (pp. 301–303). University of Chicago Press.

Hazlett, D. L. (1987). Seasonal cambial activity for *Pentaclethra*, *Goelthalsia*, and *Carapa* trees in a Costa Rican lowland Forest. *Biotropica*, *19*(4), 357. https://doi.org/10.2307/2388633

IBGE—Instituto Brasileiro de Geografia e Estatística. (2012). *Manual Técnico da Vegetação Brasileira. 2ª edição revista e ampliada. Sistema Fitogeográfico. Inventário das Formações Florestais e Campestres. Técnicas e Manejo de Coleções Botânicas. Procedimentos para Mapeamentos*. Instituto Brasileiro de Geografia e Estatística—IBGE.

INMET. (2019). *Banco de Dados Meteorológicos para Ensino e Pesquisa*. http://nmet.gov.br/portal/index.php?r=bdmep/bdmep

Junk, W. J., & Piedade, M. T. F. (2010). An introduction to South American wetland forests: Distribution, definitions and general characterization. In *Amazonian floodplain forests: Ecophysiology, biodiversity and sustainable management* (pp. 3–25). Springer. https://doi.org/10.1007/978-90-481-8725-6_1

Junk, W. J., Piedade, M. T. F., Schöngart, J., Cohn-Haft, M., Adeney, J. M., & Wittmann, F. (2011). A classification of major naturally-occurring amazonian lowland wetlands. *Wetlands*, *31*(4), 623–640. https://doi.org/10.1007/s13157-011-0190-7

Klimas, C. A., Kainer, K. A., & Wadt, L. H. O. (2007). Population structure of *Carapa guianensis* in two forest types in the southwestern Brazilian Amazon. *Forest Ecology and Management*, *250*(3), 256–265. https://doi.org/10.1016/j.foreco.2007.05.025

Köhl, M., Neupane, P. R., & Lotfiomran, N. (2017). The impact of tree age on biomass growth and carbon accumulation capacity: A retrospective analysis using tree ring data of three tropical tree species grown in natural forests of Suriname. *PLoS One*, *12*(8), e0181187. https://doi.org/10.1371/journal.pone.0181187

Kubitzki, K., & Ziburski, A. (1994). Seed dispersal in flood plain forests of Amazonia. *Biotropica*, *26*(1), 30. https://doi.org/10.2307/2389108

Lieberman, D., Lieberman, M., Hartshorn, G., & Peralta, R. (1985). Growth rates and age-size relationships of tropical wet forest trees in Costa Rica. *Journal of Tropical Ecology*, *1*(2), 97–109. https://doi.org/10.1017/S026646740000016X

Lopez, O. R., & Kursar, T. A. (2007). Interannual variation in rainfall, drought stress and seedling mortality may mediate monodominance in tropical flooded forests. *Oecologia*, *154*(1), 35–43. https://doi.org/10.1007/s00442-007-0821-0

Luize, B. G., Magalhães, J. L. L., Queiroz, H., Lopes, M. A., Venticinque, E. M., de Moraes Novo, E. M. L., & Silva, T. S. F. (2018). The tree species pool of Amazonian wetland forests: Which species can assemble in periodically waterlogged habitats? *PLoS One*, *13*(5), 1–13. https://doi.org/10.1371/journal.pone.0198130

Metzger, J. P., Bernacci, L. C., & Goldenberg, R. (1997). Pattern of tree species diversity in riparian forest fragments of different widths (SE Brazil). *Plant Ecology*, *133*(2), 135–152. https://doi.org/10.1023/A:1009791831294

Miranda, Z. P., Guedes, M. C., Rosa, S. A., & Schöngart, J. (2018). Volume increment modeling and subsidies for the management of the tree *Mora paraensis* (Ducke) Ducke based on the study of growth rings. *Trees*, *32*(1), 277–286. https://doi.org/10.1007/s00468-017-1630-7

Newbery, D. M., & Ridsdale, C. E. (2016). Neighbourhood abundance and small-tree survival in a lowland Bornean rainforest. *Ecological Research*, *31*(3), 353–366. https://doi.org/10.1007/s11284-016-1345-z

Nowacki, G. J., & Abrams, M. D. (1997). Radial-growth averaging criteria for reconstructing disturbance histories from presettlement-origin oaks. *Ecological Monographs*, *67*(2), 225–249. https://doi.org/10.1890/0012-9615(1997)067[0225:RGACFR]2.0.CO;2

Oberbauer, S. F., & Strain, B. R. (1985). Effects of light regime on the growth and physiology of *Pentaclethra macroloba* (Mimosaceae) in Costa Rica. *Journal of Tropical Ecology*, *1*(4), 303–320. https://doi.org/10.1017/S0266467400000390

Oliveira, W. S., Silva, J. A. M., & Rocha, C. A. M. (2020). Prospecção Científica e Tecnológica da Utilização do Óleo de Pracaxi. *Cadernos de Propescção*, *12*(5), 1560–1571. https://doi.org/10.9771/cp.v12i5%20Especial.32629

Parolin, P. (2002). Submergence tolerance vs. escape from submergence: Two strategies of seedling establishment in Amazonian floodplains. *Environmental and Experimental Botany*, *48*(2), 177–186. https://doi.org/10.1016/S0098-8472(02)00036-9

Parolin, P., Lucas, C., Piedade, M. T. F., & Wittmann, F. (2010). Drought responses of flood-tolerant trees in Amazonian floodplains. *Annals of Botany*, *105*(1), 129–139. https://doi.org/10.1093/aob/mcp258

Parolin, P., Simone, O., Haase, K., Waldhoff, D., Rottenberger, S., Kuhn, U., Kesselmeier, J., Kleiss, B., Schmidt, W., Piedade, M. T. F., & Junk, W. J. (2004). Central Amazonian floodplain forests: Tree adaptations in a pulsing system. *The Botanical Review*, *70*(3), 357–380. https://doi.org/10.1663/0006-8101(2004)070[0357:CAFFTA]2.0.CO;2

Parolin, P., Wittmann, F., & Ferreira, L. V. (2013). Fruit and seed dispersal in Amazonian floodplain trees—A review. *Ecotropica*, *19*(1), 19–36.

Peters, C. M. (1996). *The ecology and management of non-timber forest resources* (pp. 1–176). World Bank Group.

Pinto, E. R. (2014). *Solos, hidrologia e estrutura populacional de pracuubeiras em florestas de várzea do estuário amazônico*. Universidade Federal do Amapá.

R Core Team. (2019). *R: A language and environment for statistical computing*. Vienna, Austria. https://www.r-project.org/

Reyes, G., Brown, S., Chapman, J., & Lugo, A. E. (1992). *Wood densities of tropical tree species* [Technical report]. Forest Service.

Ripley, B. D. (1981). *Spatial statistics*. John Wiley & Sons. https://doi.org/10.1002/0471725218

Rowlingson, B., & Diggle, P. (2017). *Splancs: Spatial and space time point pattern analysis*. https://cran.r-project.org/package=splancs

Sarquis, R. D. S. F. R., Sarquis, Í. R., Sarquis, I. R., Fernandes, C. P., Silva, G. A., Silva, R. B. L., Jardim, M. A. G., Sánchez-Ortíz, B. L., & Carvalho, J. C. T. (2019). The use of medicinal plants in the riverside community of the Mazagão river in the Brazilian Amazon, Amapá, Brazil: Ethnobotanical and ethnopharmacological studies. *Evidence-based Complementary and Alternative Medicine*, *2019*, 1–25. https://doi.org/10.1155/2019/6087509

Schöngart, J. (2008). Growth-oriented logging (GOL): A new concept towards sustainable forest management in central Amazonian várzea floodplains. *Forest Ecology and Management*, *256*(1–2), 46–58. https://doi.org/10.1016/j.foreco.2008.03.037

Schöngart, J., Gribel, R., Ferreira da Fonseca-Junior, S., & Haugaasen, T. (2015). Age and growth patterns of Brazil nut trees (*Bertholletia excelsa* Bonpl.) in Amazonia, Brazil. *Biotropica*, *47*(5), 550–558. https://doi.org/10.1111/btp.12243

Schöngart, J., Piedade, M. T. F., Ludwigshausen, S., Horna, V., & Worbes, M. (2002). Phenology and stem-growth periodicity of tree species in Amazonian floodplain forests. *Journal of Tropical Ecology*, *18*(04), 581–597. https://doi.org/10.1017/S0266467402002389

Schöngart, J., Piedade, M. T. F., Wittmann, F., Junk, W. J., & Worbes, M. (2005). Wood growth patterns of *Macrolobium acaciifolium* (Benth.) Benth. (Fabaceae) in Amazonian black-water and white-water floodplain forests. *Oecologia*, *145*(3), 454–461. https://doi.org/10.1007/s00442-005-0147-8

Schöngart, J., Wittmann, F., Worbes, M., Piedade, M. T. F., Krambeck, H. J., & Junk, W. J. (2007). Management criteria for *Ficus insipida* Willd. (Moraceae) in Amazonian white-water floodplain forests defined by tree-ring analysis. *Annals of Forest Science*, *64*(6), 657–664. https://doi.org/10.1051/forest:2007044

Sillett, S. C., Van Pelt, R., Koch, G. W., Ambrose, A. R., Carroll, A. L., Antoine, M. E., & Mifsud, B. M. (2010). Increasing wood production through old age in tall trees. *Forest Ecology and Management*, *259*(5), 976–994. https://doi.org/10.1016/j.foreco.2009.12.003

Simmons, C. V., Banov, F., & Banov, D. (2015). Use of a topical anhydrous silicone base containing fatty acids from pracaxi oil in a patient with a diabetic ulcer. *SAGE Open Medical Case Reports*, *3*, 1–4. https://doi.org/10.1177/2050313X15589676

Sturges, H. A. (1926). The choice of a class interval. *Journal of the American Statistical Association*, *21*(153), 65–66. https://doi.org/10.1080/01621459.1926.10502161

ter Steege, H., Prado, P. I., Lima, R. A. F.d., Pos, E., de Souza Coelho, L., de Andrade Lima Filho, D., Salomão, R. P., Amaral, I. L., de Almeida Matos, F. D., Castilho, C. V., Phillips, O. L., Guevara, J. E., de Jesus Veiga Carim, M., López, D. C., Magnusson, W. E., Wittmann, F., Martins, M. P., Sabatier, D., Irume, M. V., … Pickavance, G. (2020). Biased-corrected richness estimates for the Amazonian tree flora. *Scientific Reports*, *10*(1), 1–13. https://doi.org/10.1038/s41598-020-66686-3

Valverde-Barrantes, O. J., & Rocha, O. J. (2014). Logging impacts on forest structure and seedling dynamics in a *Prioria copaifera* (Fabaceae) dominated tropical rain forest (Talamanca, Costa Rica). *Revista de Biologia Tropical*, *62*(1), 347–357. https://doi.org/10.15517/rbt.v62i1.8504

Wittmann, F., Anhuf, D., & Funk, W. J. (2002). Tree species distribution and community structure of central Amazonian várzea forests by remote-sensing techniques. *Journal of Tropical Ecology*, *18*(6), 805–820. https://doi.org/10.1017/S0266467402002523

Worbes, M., & Fichtler, E. (2010). Wood anatomy and tree-ring structure and their importance for tropical dendrochronology. In W. J. Junk, F. Wittmann, P. Parolin, M. T. F. Piedade, & J. Schöngart (Eds.), *Amazonian floodplain forests: Ecophysiology, biodiversity and sustainable management* (pp. 329–346). Springer Dordrecht Heidelberg London. https://doi.org/10.1007/978-90-481-8725-6_17

Ziburski, A. (1991). Dissemination, Keimung und Etablierung einiger Baumarten der Überschwemmungswälder Amazoniens. *Tropische Und Subtropische Pflanzenwelt*, *77*(1), 1–96.

How to cite this article: Dantas, A. R., Guedes, M. C., Lira-Guedes, A. C., Schöngart, J., & Piedade, M. T. F. (2022). Demographic and growth patterns of *Pentaclethra macroloba* (Willd.) Kuntze, a hyperdominant tree in the Amazon River estuary. *Population Ecology*, 1–15. https://doi.org/10.1002/1438-390X.12112